# Joint Image Reconstruction and Phase Corruption Maps Estimation in Multi-Shot Echo Planar Imaging*

Iñaki Rabanillo[1,2][0000-0001-[illegible]309-6446], Santiago Sanz-Estébanez[1,2][00[illegible]-0002-[illegible]388-0700], Santiago Aja-Fernández[1][0000-0002-5337-5071], Joseph V. Hajnal[2][0000-0002-2690-5495], Carlos Alberola-López[2][0[illegible]0-000[illegible]-3684-0055], and Lucilio Cordero-Grande[2][[illegible]003-1477-304X]

[1] Laboratorio de Procesado de Imagen, Universidad de Valladolid, Valladolid, Spain

[2] Centre for the Developing Brain and Department of Biomedical Engineering, Division of Imaging Sciences and Biomedical Engineering, King's College London, King's Health Partners, St. Thomas' Hospital, London, SE1 7EH, UK

**Abstract.** Multishot echo planar imaging is a common strategy in diffusion Magnetic Resonance Imaging to reduce the artifacts caused by the long echo-trains in single-shot acquisitions. However, it suffers from shot-to-shot phase discrepancies associated to subject motion, which can notably degrade the quality of the reconstructed image. Consequently, some type of motion-induced phases error correction needs to be incorporated into the reconstruction process. In this paper we focus on ridig motion induced errors, which have proved to corrupt the shots with linear phase maps. By incorporating this prior knowledge, we propose a maximum likelihood formulation that estimates both the parameters characterising the linear phase maps and the reconstructed image. In order to make the problem tractable, we follow a greedy iterative procedure that alternates between the estimation of each of them. Simulation data are used to demonstrate the performance of our method against state-of-the-art alternatives.

**Keywords:** Multi-shot EPI · Parallel imaging · Motion-induced phase error

## 1 Introduction

Diffusion-weighted imaging (DWI) is a non invasive technique that allows for quantification of water molecules diffusion in biological tissues. Due to its speed and insensitivity to motion, single-shot echo planar imaging (ss-EPI) has become the most commonly used sequence in DWI. However, its long echo-trains

* The authors acknowledge MICIN for grants TEC2013-44194P, TEC 2014-57428 and TEC2017-82408-R, as well as Junta de Castilla y Len for grant VA069U16. The first author acknowledges MINECO for FPI grant BES-2014-069524.

result in significant image distortions due to B0-field inhomogeneities, eddy currents, T2*-blurring or chemical shift [1]. In order to achieve higher resolution and less distortion using ss-EPI, different alternatives have been studied. One option would be to combine it with parallel imaging, but the acceleration rate is limited by the noise amplification. Another possibility would be to use reduced field-of-view (rFOV) techniques [2], where only a portion of the object is excited [3], leading to shorter echo trains as a lower resolution $\boldsymbol{k}$–space suffices to reconstruct the image. The negative aspect is that this technique is uniquely useful when we are only interested in a specific part of the object [2, 4].

A different approach to reduce the EPI echo train is multi-shot EPI (ms-EPI), which consists in segmenting the readout into multiple interleaved shots [5]. This reduces the readout duration and, as a result, the distortion caused by the aforementioned effects. However, phase inconsistencies between different shots induced by subject motion may cause additional ghost artifacts. For this reason, ms-EPI sequences need to incorporate a phase-correction technique that accounts for these phase mismatches between shots.

Subject-induced phase maps in ms-EPI behave similarly to sensitivity maps in parallel imaging (PI) in the sense that they can be modelled as a pixelwise multiplication between the original image and corresponding map. This analogy motivates the translation of PI techniques to reconstruct the multi-shot data under shot-to-shot phase discrepancies. State-of-the-art methods can be classified into three different groups: navigated methods, self–navigated methods and navigator–free methods. The first group relies on the acquisition of callibration data from where the phase-maps can be estimated and incorporated into a SENSE-type reconstruction [6], but they are not able to deal with dynamic errors, i.e., mismatches between the navigator and the imaging data. For that purpose, self–navigated methods acqure the callibration data within the imaging sequence, and further reconstruct the image based on different PI techniques such as GRAPPA [7], SPIRiT [8] or LORAKS [9]. However, this approach is time-inefficient, which led to the developement of techniques that retrospectively correct for ghosting artifacts from the images themselves using priors such as phase smoothness [10], rigid–motion [6] or low-rankness [11].

In this paper, we present a navigator-free method to reconstruct ms-EPI images under the assumption of intra-shot rigid motion. Anderson et. al. proved that the resulting phase errors are linear in the image space, which turn into shifts and constant offsets in $\boldsymbol{k}$–space [5]. Incorporating this knowledge into the model, we present an image reconstruction procedure based on the optimization of a functional used to jointly estimate the $\boldsymbol{k}$–space shifts and offsets and the diffusion image by exploiting the sensitivity encoding [12] redundancy provided by the the coil array. This philosophy has already proven succesful for the correction between even and odd lines, where corruption occurs only along the fully–sampled readout direction [13].

## 2 Theory

### 2.1 Problem formulation

Under the assumption of rigid motion during the application of diffusion-sensitized gradients the phase corruption for each shot becomes linear and can be characterized by three parameters in 2D imaging. Thus, the reconstruction for parallel multishot imaging can be performed by means of the maximum likelihood formulation in matrix form as:

$$(\mathbf{x}^*, \theta^*) = \operatorname*{argmin}_{\mathbf{x},\theta} \|\boldsymbol{A}\boldsymbol{\mathcal{F}}\boldsymbol{S}\boldsymbol{\mathcal{P}}(\theta)\boldsymbol{x} - \boldsymbol{y}\|_2^2 . \tag{1}$$

The aim is to reconstruct a 2D image (although the model could be easily generalized to 3D imaging) $\boldsymbol{x}$ of size $N = N_1 \cdot N_2$, where $N_l$ refers to the number of voxels along the dimension $l$ using an array containing $C$ coils from $M = E \cdot S \cdot C$ samples of a discretized $\boldsymbol{k}$–space grid of size $K = K_1 \cdot K_2$. $E$ refers to the number of sampled points per shot and $S$ is the number of shots. The terms in (1) are represented by the following matrices:

- $\boldsymbol{y}$ is a vector of size $M \times 1$ containing measured multi-shot $\boldsymbol{k}$–space data.
- $\boldsymbol{A}$ is a sampling matrix of size $M \times KSC$ given by

$$\boldsymbol{A} = \begin{pmatrix} \boldsymbol{A}_{11} & \cdots & & \cdots & \mathbf{0} \\ \vdots & \ddots & \vdots & \vdots & \vdots \\ \mathbf{0} & \cdots & \boldsymbol{A}_{1C} & \cdots & \mathbf{0} \\ \vdots & \vdots & \vdots & \ddots & \vdots \\ \mathbf{0} & \cdots & \mathbf{0} & \cdots & \boldsymbol{A}_{SC} \end{pmatrix}, \tag{2}$$

  where $A_{sc}$ is a matrix of size $E \times K$ whose entries are equal to 1 if the sample $e$ of the shot $s$ matches the $\boldsymbol{k}$–space location indexed by $k$ and 0 otherwise.
- $\boldsymbol{\mathcal{F}}$ is a matrix of size $KSC \times NSC$ that performs the Discrete Fourier Transform (DFT) given by the diagonal block structure

$$\boldsymbol{\mathcal{F}} = \begin{pmatrix} \boldsymbol{F}_{11} & \cdots & & \cdots & \mathbf{0} \\ \vdots & \ddots & \vdots & \vdots & \vdots \\ \mathbf{0} & \cdots & \boldsymbol{F}_{1C} & \cdots & \mathbf{0} \\ \vdots & \vdots & \vdots & \ddots & \vdots \\ \mathbf{0} & \cdots & \mathbf{0} & \cdots & \boldsymbol{F}_{SC} \end{pmatrix}, \tag{3}$$

  where $F_{sc}$ is a $K \times N$ matrix performing the 2D DFT.
- $\boldsymbol{S}$ is a matrix of size $NSC \times NS$ containing properly arranged coil sensitivity maps:

$$\boldsymbol{S} = \begin{pmatrix} \boldsymbol{S}_{11} & \cdots & \mathbf{0} \\ \vdots & \ddots & \vdots \\ \boldsymbol{S}_{1C} & \cdots & \mathbf{0} \\ \vdots & \ddots & \vdots \\ \mathbf{0} & \cdots & \boldsymbol{S}_{SC} \end{pmatrix}, \tag{4}$$

where $S_{sc}$ is a diagonal matrix of size $N \times N$ containing the sensitivity profile of coil $c$.

- $\boldsymbol{\mathcal{P}}(\theta)$ is a matrix of size $NS \times N$ containing the phase maps given by

$$\boldsymbol{\mathcal{P}}(\theta) = \begin{pmatrix} \boldsymbol{P}(\theta_{\mathbf{1}}) \\ \vdots \\ \boldsymbol{P}(\theta_{\mathbf{S}}) \end{pmatrix}, \tag{5}$$

where $\boldsymbol{P}(\theta_{\mathbf{s}})$ is a diagonal matrix of size $N \times N$ containing the linear phase map for shot $s$ characterized by three parameters $\theta_{\mathbf{s}} = [\theta_{s0}\theta_{s1}\theta_{s2}]$. Its diagonal is given by the vector $p_s(\theta_{\mathbf{s}})$:

$$p_s(\theta_{\mathbf{s}}) = e^{i(\theta_{s0}+\theta_{s1}\cdot r_1+\theta_{s2}\cdot r_2)}, \tag{6}$$

where $r_l$ denotes the spatial coordinate vector along dimension $l$.

- $\boldsymbol{x}$ is a vector of size $N \times 1$ containing the reconstructed image.

### 2.2 Problem solving

Our minimization problem is a non-linear least squares optimization problem, which does not have a closed-form solution in general. Directly solving the joint optimization problem, however, is practically intractable. For this reason, we proceeded in a greedy iterative fashion, alternating between solving the following two subproblems [14]:

- Image reconstruction problem

$$\mathbf{x}^* = \arg\min_{\boldsymbol{x}} \|\boldsymbol{A}\boldsymbol{\mathcal{F}}\boldsymbol{S}\boldsymbol{\mathcal{P}}(\theta^*)\boldsymbol{x} - \boldsymbol{y}\|_2^2 \,. \tag{7}$$

This formulation is equivalent to the one of SENSE (Pruessmann), which we solve by the iterative conjugate gradient method described in (Pruessmann).

- Phase maps estimation

$$\theta^* = \arg\min_{\theta} \|\boldsymbol{A}\boldsymbol{\mathcal{F}}\boldsymbol{S}\boldsymbol{\mathcal{P}}(\theta)\boldsymbol{x}^* - \boldsymbol{y}\|_2^2 \,. \tag{8}$$

We look for the solution that nulls the gradient of the objective function and for that puporse we have chosen to use the Newton's algorithm, which uses information of the Hessian.

Since the objective function is nonconvex, it will in general contain multiple local minima. For this reason, a proper initialization becomes vital for our algorithm to find the global minimum. Taking into account that the constant offsets are preserved in $\boldsymbol{k}$–space and that linear phases introduce $\boldsymbol{k}$–space shifts, we find an initial estimate of our phase maps parameters by finding the position and phase of the peak of the spectrum. However, since each shot is undersampled by a factor equivalent to the number of shots, the peak may have been shifted to an unacquired line. Consequently, prior to peak detection, we compute an $L2$-Tikhonov regularized SENSE reconstruction of each shot. This way, we take advantage of the ideas behind methods such as MUSE, although we could use other kind of regularizations (low-rank as in MUSSELS, for example) as well.

Nevertheless, this initialization will be subject to a certain degree of uncertainity in the detection of the peak if the reconstructed shots show a large noise amplification or ghosting. For this reason, and to help Newton's method scape from local minima, we search in a discretized grid in the space of phases for each shot around the previous phase candidates. In order to alleviate the computational burden, we decrease the size of the grid by a factor of 2 at each iteration.

## 3 Methods

With the aim of replicating the phase maps generated by a rigid motion, we used a $T_2$ neonatal brain axial image acquired with a fast spin echo sequence on a $3T$ PHILIPS ACHIEVA TX with a head coil array of 32 channels and using the following parameters: resolution= $0.8 \times 0.8mm$, slice thickness= $1.6mm$, echo time $T_E = 145ms$, repetition time $T_R = 12s$, flip angle $\alpha = 90°$. Coil sensitivity profiles were estimated from a separate prescan using (Allison). The image was reconstructed without zero filling in order to preserve the resolution and then cropped to a $128 \times 128$ matrix so the brain adjustes to the FOV. To generate our synthetic msEPI data, we applied the forward model described in Eq.(1).

We have compared our algorithm with three different alternatives:

1. MUSE [10]: we reconstruct each shot using SENSE and from it we get an estimate of its phase map after applying a Total-Variation (TV) filter. We then reconstruct the image solving the SENSE-type problem in Eq.(7).
2. Linearly parameterized MUSE (LinMUSE): since the original MUSE implementation was developed for a more general scenario where the only prior knowledge about the phase is that it is smooth, we implemented a MUSE version that incorporates the prior knowledge of linear phase corruption maps. The difference with the previous algorithm is that, instead of taking the phase of each shot-reconstructed image after the TV-filter, we estimate the three parameters caracterising the linear phase map from the peak and position of the $\boldsymbol{k}$–space peak.
3. LinMUSE with $L2-$Tikhonov regularization (LinMUSE+Tik): the presence of noise can affect the detection of the peak in $\boldsymbol{k}$-space, specially when the phase map shifted it to the furthest position from the acquired lines, i.e., to the intermediate position in between two lines for the considered shot. For this reason, a certain degree of regularization can help avoid misidentifying the peak as amplified noise. It is important to notice that a regularization may induce errors as well due to incorrect removal of ghosting artifacts.

Finally, we carried out two experiments on our data:

- In order to visually assess the ability of the aforementioned methods to reconstruct the image, we compared the reconstructions at a low SNR scenario for 4, 6 and 8 shots. The phase offset was randomly generated between $[-\pi, \pi]$, whereas the linear ramp was generated to shift the peak in the region covering the central $S$ lines. We focused on this region of linear shifts since the worst scenario arises when the peak moves to the intermediate position between two acquired lines. With respect to the acquired lines, it does not seem to matter how far away we move from the original center.
- We carried out 100 reconstructions using $S = 8$ shots for varying levels of SNR. We computed the SNR as the mean absolute signal divided by the standard deviation of the synthetic randomly gaussian added noise. The phase parameters were generated as in the previous experiment. We compared the absolute error in the estimation of the phase parameters, since they are the ones causing the ghosting artifacts in the reconstructed image.

## 4 Results

In Fig.1 we show the reconstructed images for a low SNR scenario varying the number of shots. The first column shows the ground-truth, and the next columns show the reconstruction for the described method, LinMUSE, LinMUSE+Tik and standard MUSE.

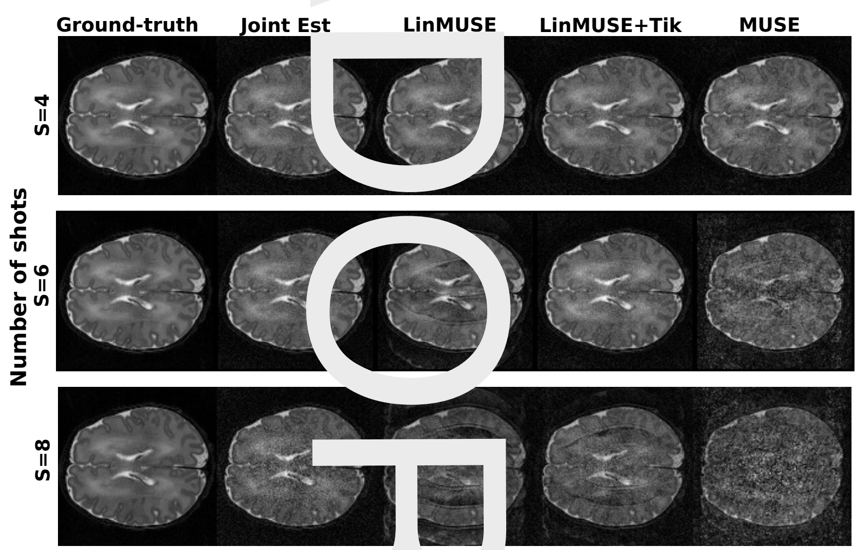


**Fig. 1.** Reconstructed images in a low SNR scenario for different number of shots: 4 (first row), 6 (second row) and 8 (third row). First column shows the ground-truth and the following ones the reconstructed images with our method (second column), LinMUSE (third column) LinMUSE+Tikhonov regularization (fourth column) and standard MUSE (fifth column).

We observe that for $S = 2$, all reconstructions seem to perform similarly, which is consistent with the literature [10]. However, when we increase the number of shots, we start to observe how the MUSE-type reconstructions introduce ghosting artifacts. For a higher number of shots, the $g$-factor noise amplification associated to SENSE becomes very high, increasing the uncertainity in the detection of the peak of the spectrum. Specifically, when the phase corruption shifts the peak to the intermediate position between two sampled lines for a particular shot, it becomes more likely to identify it at a noisy location.

We can observe as well that when an $L2$ Tikhonov regularization is applied together with SENSE, the peak detection seems to provide a good estimate of the linear phase maps parameters (see fourth column for 6 shots). By applying this regularization, we limit the noise amplification in the SENSE reconstructed shot, although the trade-off is that the reconstructed image can still show some ghosting artifacts. For this reason, we chose it as the initialization for our method, which after the steps described in the Theory Section seems to be able to provide a ghosting artifacts free image for the case of 8 shots.

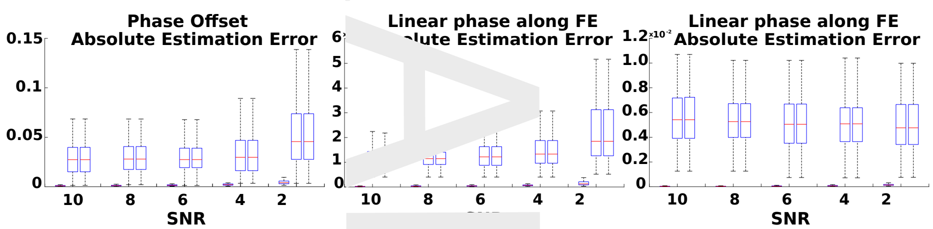


**Fig. 2.** Bosplots of the absolute errors for the phase parameters estimation: offset (first column), FE slope (second column) and PE slope (third column). We must point out that multiple outliers were present for the lowest SNR scenario in all of the studied reconstructions, although we removed them from the figure for a more clear visualization.

On the other hand, in Fig.2 we can see that the absolute errors for the estimation of the three different parameters: the constant offset, the slope along the frequency–encoding (FE) direction and the slope along the phase–encoding (PE) direction. We compared them between our method, LinMUSE and LinMUSE+Tik for varying levels of SNR. We observe that our method is always able get a closer estimate to the true phase parameters. This is consistent with the fact that our method is initialized with the phase estimates provided by LinMUSE+Tik and from there a finer estimation is done based on both the initial grid search and the subsequent Newton's method based descent.

## 5 Discussion

In this work we have proposed a joint procedure to both reconstruct the images and estimate the phase error maps for ms-EPI under the assumption of rigid motion during the application of the diffusion-sensitized gradients in dMRI. Our method is initialized with the solution provided by a linearly parametrized MUSE reconstruction that identifies the position and phase of the peak of the spectrum. By using alltogether the information from all the shots and due to the availability of multi–channel data, we are able to obtain a finer estimation of the phase parameters that results in a better removal of ghosting artifacts.

We have illustrated the performance of the proposed technique with simulations varying the number of shots and the level of noise. Importantly, our method seems able to reconstruct the images for higher number of shots compared to the considered alternatives.

This study presents some limitations. First, we have only tested the method in a synthetic phantom corrupted by linear phase maps. We expect this assumption to be a reasonable one for [illegible] of the brain, or if cardiac triggering is used during the acquisition to limit the non-linear phase effects of pulsatile motion [15]. For this reason, we believe the results are promising regarding its applicability to clinical scenarios. Second, we have only compared our method to our own implementation of MUSE [illegible] and a linearly parametrized version of it. These methods however contain different parameters that need to be tunned, so a more detailed of them should be considered to guarantee a fair comparison. Furthermore, other more complex algorithms such as LORAKS [9] or MUSSELS Mani17 could be considered as well. Third, we have just considered the case of linear phase errors, but it would be interesting to study a non-linear model based on B-splines similar to [14] that can deal with non-rigid motion. Fourth, we have only considered tha case of cartesian sampling, but our formulation is compatible with different trajectories such as spirals, so it would be interersting to test it under different sampling patterns.

## 6 Conclussions

We have developed a method that builds upon state-of-the-art techniques and is able to better estimate the phase maps corruption multi-shot EPI acquisitions, resulting in an increased ability to remove ghosting artifacts from the reconstructed images. Under the assumption of rigid motion, we pose a joint formulation that is able to both reconstruct the images and estimate the phase maps in a greedy iterative fashion.

## References

1. Jaermann T., Pruessmann K.P., Valavanis A., Kollias S. Boesiger P.: "Influence of SENSE on image properties in high-resolution diffusion tensor imaging". Magn. Res. Med. **55**(2), 335–342 (20[illegible])
2. Saritas E.U., Cunningham C.H., Lee J.H., Han E.T., Nishimura D.G.: "DWI of the spinal cord with reduced FOV singleshot EPI". Magn. Res. Med. **60**(2), 468–473 (2008)
3. Pauly J., Nishimura D.G., Macovski A.: "A k-space analysis of small-tip-angle excitation". J. Magn. Res. **81**(1), 43–56 (1989)

4. Mannelli L., Fung M.M., Ny  an G., Lope  S., Do R.K.G.: "Feasibility Study on Reduced FOV Diffusion Ima  ng of the Panc  as Using Navigator Triggering Technique". In: 23rd Annual Me  ing Internation  Society for Magnetic Resonance in Medicine Proceedings, pp. 14   Toronto, Ca  da (2015)
5. Anderson A.W., Gore J.C.: "A  rrection of motion artifacts in diffusion weighted imaging". Magn. Res. Med. **32**(3), 379–387 (1994)
6. Van A.T., Hernando D., Sutton B.P.: "Motion-Induced Phase Error Estimation and Correction in 3D Diffusion T  aging  IEEE Trans. on Med. Imag. **30**(11), 1933–1940 (2011)
7. Liu W., Zhao X., Ma Y., Tang X.,  ao J.H  "DWI Using Navigated Interleaved Multishot EPI with Realigned GRA  PA Re  nstruction". Magn. Res. Med. **75**(1), 280–286 (2016)
8. Dong Z., Wang F., Ma X., Zhang Z., Dai E., Yuan C., Guo H.: "Interleaved EPI Diffusion Imaging Using SPI  truction With Virtual Coil Compression". Magn. Res. Med. **79**(3), 1525-  531 (2  8)
9. Lobos R.A., Kim T.H., Hoge W.S., H  ldar J.  : "Navigator-free EPI Ghost Correction with Structured Low-Rank Mat  x Mod  s: New Theory and Methods". IEEE Trans. on Med. Imag. In Press (201  )
10. Chen N.K., Guidon A., Cha  g H.C., Song A.W.: "A robust multi-shot scan strategy for high-resolution diffus  on weighted MRI enabled by multiplexed sensitivity-encoding (MUSE)". Neuroimag  41–47 (2013)
11. Mani M., Jacob M., Kelley D., M  gh  V.: "Multi-shot sensitivity-encoded diffusion data recovery using struct  ed low  k matrix completion (MUSSELS)". Magn. Res. Med. **78**(2), 494–507 (  )
12. Pruessmann K.P., Weiger M  cheidegger M.B., Boesiger P.: "SENSE: Sensitivity encoding for fast MRI". Magn. Res. Med. **42**(5), 952–962 (1999)
13. Ianni J.D., Welch E.B., Gris  t reduction in echoplanar imaging by joint reconstruction of image  and linetoline  elays and phase errors". Magn. Res. Med. **79**(6), 3114–3121 (2018
14. Ying L., Sheng J.: "Joint ima  e reconstructi  and sensitivity estimation in SENSE (JSENSE)". Magn. Res. Med.  (6), 119  202 (2007)
15. Miller K., Pauly J.M.: "Nonlinear phase correction for navigated diffusion imaging". Magn. Res. Med. **50**(2), 343-35  (2003)